ORIGINAL ARTICLE

Faim2 contributes to neuroprotection by erythropoietin in transient brain ischemia

Daniel Komnig,*,[1] Karen Gertz,†,‡,[1] Pardes Habib,* Kay W. Nolte,§
Tareq Meyer,¶ Marc A. Brockmann,** Matthias Endres,†,‡,††,‡‡,§§
Birgit Rathkolb,¶¶,***,††† Martin Hrabě de Angelis,¶¶,†††,‡‡‡
German Mouse Clinic Consortium, Jörg B. Schulz,*,§§§
Björn H. Falkenburger*,§§§,[1] and Arno Reich*,[1]

*Department of Neurology, RWTH Aachen University, Aachen, Germany

†Department of Neurology, Charité Universitätsmedizin Berlin, Berlin, Germany

‡Center for Stroke Research Berlin, Charité Universitätsmedizin Berlin, Berlin, Germany

§Institute of Neuropathology, RWTH Aachen University, Aachen, Germany

¶Department of Diagnostic and Interventional Neuroradiology, University Hospital RWTH Aachen,
Aachen, Germany

**Department of Neuroradiology, University Medical Centre of the Johannes Gutenberg University
Mainz, Mainz, Germany

††Excellence Cluster NeuroCure, Berlin, Germany

‡‡German Center for Neurodegenerative Disease (DZNE), Berlin, Germany

§§German Center for Cardiovascular Research (DZHK), Berlin, Germany

¶¶German Mouse Clinic, Institute of Experimental Genetics, Helmholtz Zentrum München, German
Research Center for Environmental Health GmbH, Neuherberg, Germany

***Ludwig-Maximilians-Universität München, Gene Center, Institute of Molecular Animal Breeding
and Biotechnology, München, Germany

†††German Center for Diabetes Research (DZD), Neuherberg, Germany

‡‡‡Chair of Experimental Genetics, Center of Life and Food Sciences Weihenstephan, Technische
Universität München, Freising-Weihenstephan, Germany

§§§JARA-BRAIN Institute Molecular Neuroscience and Neuroimaging, Forschungszentrum Jülich
GmbH and RWTH Aachen University, Aachen, Germany

Abstract

Delayed cell death in the penumbra region of acute ischemic stroke occurs through apoptotic mechanisms, making it amenable to therapeutic interventions. Fas/CD95 mediates apoptotic cell death in response to external stimuli. In mature neurons, Fas/CD95 signaling is modulated by Fas-apoptotic inhibitory molecule 2 (Faim2), which reduces cell death in animal models of stroke, meningitis, and Parkinson disease. Erythropoietin (EPO) has been studied as a therapeutic strategy in ischemic stroke. Erythropoietin stimulates the phosphatidylinositol-3 kinase/Akt (PI3K/Akt) pathway, which regulates Faim2 expression. Therefore, up-regulation of Faim2 may contribute to neuroprotection by EPO. Male Faim2-deficient mice (Faim2$^{-/-}$) and wild-type littermates

ORIGINAL ARTICLE

(WT) were subjected to 30 min of middle cerebral artery occlusion (MCAo) followed by 72 h of reperfusion. EPO was applied before (30 min) and after (24 and 48 h) MCAo. In WT mice application of EPO at a low dose (5000 U/kg) significantly reduced stroke volume, whereas treatment with high dose (90 000 U/kg) did not. In Faim2$^{-/-}$ animals administration of low-dose EPO did not result in a significant reduction in stroke volume. Faim2 expression as measured by quantitative reverse transcription polymerase chain reaction (qRT-PCR) increased after low-dose EPO but not with high dose. An extensive phenotyping including analysis of cerebral vessel architecture did not reveal confounding differences between the genotypes. In human post-mortem brain Faim2 displayed a differential expression in areas of penumbral ischemia. Faim2 up-regulation may contribute to the neuroprotective effects of low-dose erythropoietin in transient brain ischemia. The dose-dependency may explain mixed effects of erythropoietin observed in clinical stroke trials.

Keywords: dose-dependency, erythropoietin, Fas-apoptotic inhibitory molecule 2, ischemia-reperfusion, neuroprotection, stroke.

J. Neurochem. (2018) https://doi.org/10.1111/jnc.14296

Acute ischemic stroke is a major source of morbidity and mortality with an increasing incidence and prevalence worldwide (Kim *et al.* 2015). Immediate, irreversible neurological damage occurs in the infarct core, where absolute oxygen and glucose deprivation result in a rapid loss of function and structure (i.e., necrotic cell death). In the adjacent penumbra relative oxygen and glucose deprivation because of varying collateral supply lead to delayed and potentially reversible apoptotic cell death (Pundik *et al.* 2012; Sanderson *et al.* 2013).

Fas/CD95 contributes to apoptotic neuron death in the ischemic brain (reviewed, e.g., in Reich *et al.* 2008). Several animal models of focal cerebral ischemia demonstrated regulation of Fas/CD95, its ligand FasL/CD95L and downstream caspases (caspase-8 and caspase-3) (Reich *et al.* 2011; Lu *et al.* 2012; Chelluboina *et al.* 2014). Fas/CD95-mediated apoptosis can be inhibited by Fas-apoptotic inhibitory molecule 2 (Faim2) (Schweitzer *et al.* 1998; Somia *et al.* 1999; Fernandez *et al.* 2007). Alternative names for Faim2 are Lifeguard (LFG), Lifeguard 2 (LFG2), transmembrane BAX inhibitor motif containing 2 (TMBIM2) and neuronal membrane protein 35 (NMP35). Faim2 is neuroprotective in cell culture and mouse models of transient cerebral ischemia (Reich *et al.* 2011), retinal detachment (Besirli *et al.* 2012), pneumococcal meningitis (Tauber *et al.* 2014), and Parkinson disease (Komnig *et al.* 2016).

Erythropoietin (EPO) is a 30.4 kDa glycoprotein, which stimulates erythropoiesis and is used as a treatment for anemia (Fisher 2010). Systemically administered EPO can cross the disrupted blood-brain barrier in stroke and has repeatedly been shown to reduce infarct volumes in animal models of ischemic stroke (Brines *et al.* 2000; Siren *et al.* 2001; Villa *et al.* 2003; Yu *et al.* 2005; Wakida *et al.* 2007; Wang *et al.* 2007; Minnerup *et al.* 2009). Mechanistically, EPO attenuates apoptotic neuronal death, cytokine production and inflammation in rat models of ischemia (Villa *et al.* 2003; Wang *et al.* 2007). The amount of EPO given has varied over a wide range. Three doses of 5000 U/kg reduce infarct size in a rat model of embolic stroke using transient middle cerebral artery occlusion (MCAo) (Wang *et al.* 2007). In mice subjected to permanent MCAo, pretreatment with EPO doses ranging from 3×3000 U/kg to $3 \times 30 000$ U/kg (applied 24 h before, 1 h before, and just after MCAo), reduces cortical infarct volume only with high doses (Wakida *et al.* 2007).

A double-blind randomized proof-of-concept clinical trial in 80 stroke patients showed improved functional outcome at day 30, when EPO was administered up to 8 h after an ischemic stroke within the middle cerebral artery territory (Ehrenreich *et al.* 2002). However, a follow-up study in 522 patients failed to reproduce beneficial effects of EPO administration and raised concerns about its safety (Ehrenreich *et al.* 2009).

The signaling pathway by which EPO protects neurons in cerebral ischemia has not been resolved. Kilic *et al.* (2005) subjected transgenic mice with constitutively expressed human EPO to severe (90 min) and mild (30 min) MCAo and found that EPO expression protects mouse brain accompanied by a dual activation of extracellular signal-regulated kinase 1 and 2 (ERK-1/-2) and phosphatidylinositol-3 kinase/Akt (PI3K/Akt) pathways downstream of EPO (Kilic *et al.* 2005). An activation of PI3K was also found in other studies (Chateauvieux *et al.* 2011).

Given that activation of PI3K/Akt pathway regulates Faim2 expression (Brunet *et al.* 2001; Beier *et al.* 2005), and our previous finding that Faim2 protects against ischemic cell death in mice and cultured cells (Reich *et al.* 2011), we hypothesize that Faim2 is involved in EPO-mediated neuroprotection. This hypothesis was tested in an animal model of transient cerebral ischemia. Because a wide range of EPO concentrations has been described, we used two dosages, 5000 and 90 000 U/kg administered at three time points. In addition, we measured Faim2 expression in response to EPO administration and evaluated Faim2 expression in samples of the penumbra region of human patients with ischemic stroke.

Methods

Animals

All mice were housed and handled according to guidelines from the Federation for European Laboratory Animal Science Associations (FELASA) in a pathogen-free facility in a temperature-controlled room (20–24°C) with a 12 h light/dark cycle and food and water *ad libitum*. The animal experiments were approved by the District Government of North Rhine Westphalia in Recklinghausen, Germany. Male Faim2 null mutants (Faim2$^{-/-}$) and wild-type littermates (Faim2$^{+/+}$) were 10–12 weeks of age at the beginning of the experiments. Generation of the Faim2 null mutants was described previously (Reich *et al.* 2011). Faim2 null mutants were backcrossed to C57BL/6J (IMSR Cat# JAX:000664, RRID:IMSR_JAX:000664) background for more than eight generations.

Model of cerebral ischemia

Transient cerebral ischemia was induced by intraluminal occlusion of the left middle cerebral artery (MCA) for 30 min as described previously (Kilic *et al.* 2002; Reich *et al.* 2011; Gertz *et al.* 2012). In brief, mice were anaesthetized with 1.5% isoflurane (Forene; Servopharma GmbH, Oberhausen, Germany) and maintained in 1% isoflurane in 69% N_2O and 30% O_2. The ischemic insult was induced by an 8.0 nylon monofilament (Doccol Cat# 801912PK5, MA, USA) coated with a silicone resin/hardener mixture (Xantopren M Mucosa and Activator NF Optosil, both Heraeus Kulzer). The monofilament was introduced into the internal carotid artery up to the anterior cerebral artery. Thereby, the MCA and anterior choroidal arteries were occluded. The filament was removed 30 min after occlusion to allow reperfusion. For pain relief bupivacaine gel was topically applied in the wound. Core temperature was maintained at 36.5 ± 0.5°C with a feedback temperature control unit during MCA occlusion.

As part of its quality management system, the Department of Experimental Neurology at Charité Berlin has established detailed standard operating procedures (Ulrich Dirnagl and Members of the MCAo SOP group; Nature Precedings, 2012). In order to reduce animal number and suffering, MCAo surgeons need to demonstrate their ability to perform the MCAo procedure with a high degree of reproducibility.

EPO treatment

Erythropoietin (Epoetin alfa Hexal, Hexal, Holzkirchen, Germany) was diluted in 0.9% NaCl and 3 doses of 5000 U/ kg body weight or 90 000 U/kg were injected i.p. (Fig. 1a). In the stroke model, EPO was administered 30 min before, 24 and 48 h after MCAo (cumulative EPO doses 15 000 U/ kg or 270 000 U/kg, respectively). Controls were injected with saline only (vehicle).

Histological analysis of injury and determination of hematocrit values

After 72 h reperfusion mice were deeply anesthetized (isoflurane) and sacrificed by decapitation. Blood was sampled in heparinized hematocrit capillaries. After centrifugation at 2300 g for 10 min, the packed red cells were separated from the plasma and the length of the fractions was measured. The hematocrit was calculated by division of the packed red blood cell fraction by the total fraction of the blood sample.

Brains were snap-frozen in isopentane (−45°C) and stored at −80°C until cryostat sectioning. Ischemic lesion sizes were analyzed from serial 20 µm-thick hematoxylin stained coronal brain sections (2 mm apart) as described (Yildirim *et al.* 2014). Infarct sizes were determined with an image analysis system (SigmaScan Pro 5.0; SYSTAT, San Jose, CA, USA) and calculated by summing the volumes of each section directly.

Quantitative reverse transcription polymerase chain reaction (qRT–PCR)

Twelve-week-old male mice were sacrificed under deep isoflurane anesthesia by decapitation for evaluating gene expression in the brain. EPO receptor (EPO-R) expression was analyzed in Faim2 knockout mice and wild-type littermates (Faim2$^{+/+}$: $n = 7$; Faim2$^{-/-}$: $n = 7$). Faim2 expression was evaluated in wild-type mice 12 h after a single EPO dose or vehicle treatment (5000 U/kg EPO: $n = 6$; 90 000 U/kg EPO: $n = 6$; vehicle: $n = 6$). After decapitation, cortex and midbrain were rapidly dissected on ice and quick-frozen in liquid nitrogen. RNA was isolated using TRIzol® Reagent (Invitrogen Cat# 15596-026, Carlsbad, CA, USA). Total RNA (500 ng) was reverse-transcribed by iScript™ Reverse Transcription Supermix (Bio-Rad Laboratories Cat# 170-8891SP, Munich, Germany) according to the manufacturer's instructions. cDNA was diluted 1 : 12.5 with diethylpyrocarbonate water and amplified using SYBR® Green (Bio-Rad Laboratories Cat# 170-8884). Annealing temperature was set to 60°C. Quantification was performed with the MyiQ2 Two-Color Real-Time PCR Detection System (Bio-Rad Laboratories) based on triplicates per primer set for each animal. RNA expression was normalized to murine glyceraldehyde 3-phosphate dehydrogenase (GAPDH) as housekeeping gene. Relative gene expression was calculated using the delta-delta cycle threshold method. The following forward (fwd) and reverse (rev) primers were used (5′->3′): GAPDH fwd: CCTTCTGACACGGATTTGGT; GAPDH rev: ACATC-GAGATCGCCACCTAC; Faim2 fwd: AGAAGACATCAT-GACCCAGGG; Faim2 rev: CTTTCTGGTCATCCC AGCTG, as previously (Komnig *et al.* 2016) and EPO-R fwd: CTCACCTTCCAGCTTTGAGT, EPO-R rev: TTCTCATAGGGGTGGGAGTA. Primer pair specificity was validated by analyzing qRT-PCR samples via agarose
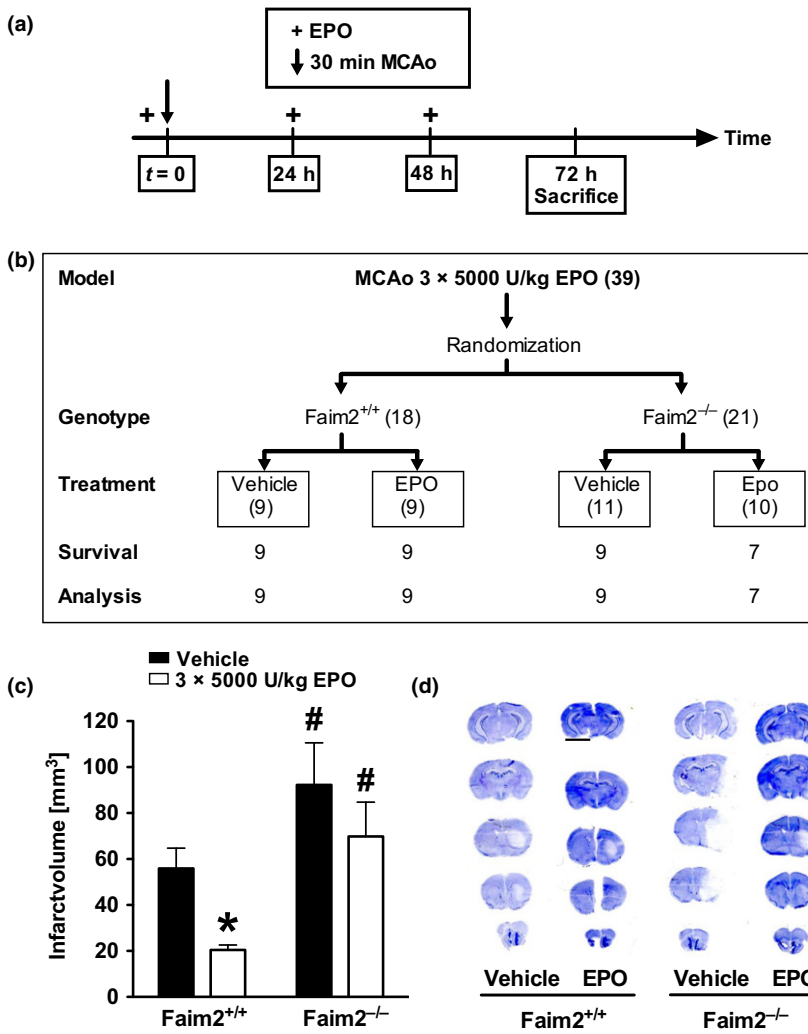
Fig. 1 Acute lesion size after 3 × 5000 U/kg EPO. (a) Faim2$^{-/-}$ and wild-type litter-mates (Faim2$^{+/+}$) were treated i.p. with erythropoietin (EPO) in a dose of 5000 U/kg body weight or vehicle alone. Treatment was performed 30 min before, and 24 and 48 h after middle cerebral artery occlusion (MCAo). (b) Summary of the number of total animals per group for final analyses. (c and d) Acute neuronal damage was assessed at 72 h after 30 min MCAo/reperfusion using hematoxylin standard histochemistry. Direct cerebral lesion volumes were determined on five coronal brain sections (approximately interaural 6.6, 5.3, 3.9, 1.9, and −0.1 mm, respectively) by computer-assisted volumetry. Representative images of hematoxylin histochemistry are presented in (d). Number of animals that completed the experiment: vehicle Faim2$^{+/+}$: $n = 9$; vehicle Faim2$^{-/-}$: $n = 9$; EPO-treated Faim2$^{+/+}$: $n = 9$; EPO-treated Faim2$^{-/-}$: $n = 7$. Data shown as mean ± SEM, two-way ANOVA followed by Newman-Keul's *post hoc* test, *$p < 0.05$ relative to vehicle treatment within genotype, #$p < 0.05$ relative to wild-type within treatment, scale bar 5 mm.

gel electrophoresis resulting in a single band per gene of interest (not shown).

Digital subtraction angiography (DSA) and micro–CT imaging

Faim2$^{-/-}$ ($n = 5$) and Faim2$^{+/+}$ mice ($n = 4$) were anesthetized by i.p. administration of ketamine (100 mg/kg body weight) and xylazine (5 mg/kg body weight). Digital subtraction angiography (DSA) and Micro-Computed Tomography (Micro-CT) were performed as recently described (Schambach *et al.* 2009; Figueiredo *et al.* 2012). Briefly, an industrial micro-CT (Xylon Y.Fox; Yxlon International, Hamburg, Germany) equipped with a transmission X-ray tube and an amorphous silicon flat panel detector (1888 × 1408 pixels; Varian PaxScan 2520; Varian, Palo Alto, CA, USA) was used. The tail vein was catheterized, the mouse was fixed in an acrylic cradle and placed within the path of the X-ray beam within the micro-CT. Undiluted pre-warmed contrast agent (Iomeprol 300;

Bracco Imaging, Konstanz, Germany) was injected intra-venously (DSA: 200 μL, micro-CT: 300 μL) using an infusion pump (PHD 2000; Harvard Apparatus, March-Hugstetten, Germany). DSA was performed at 80 kilovolt with the detector pixel matrix set to 944 × 704 (2 × 2 binning) at 30 frames per second. The tube current was maximized to optimize the signal to noise ratio while preventing overexposure of the detector. The source-object distance and object-detector distance were adjusted so that the entire cerebral circulation of the mouse could be visualized within the field of view. For DSA, gain-offset calibration was performed before contrast injection. DSA sequences were recorded digitally in an AVI movie file format.

Micro-CT was performed with continuous image acquisition at 30 frames per second during a 190° rotation of the animal within 40 s (total of 1200 projections per scan). Each scan was commenced 5 s after starting contrast agent injection. The images were reconstructed using the software
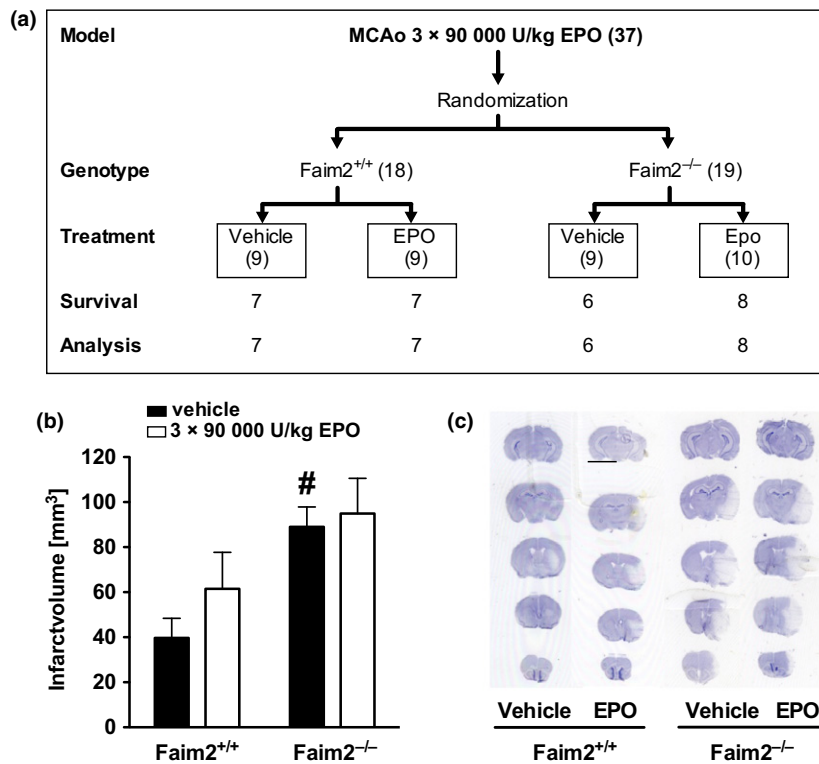
Fig. 2 Acute lesion size after 3 × 90 000 U/kg EPO. (a) Summary of the number of total animals per group for final analyses. Faim2$^{-/-}$ and wild-type littermates (Faim2$^{+/+}$) were treated i.p. with erythropoietin (EPO) in a dose of 90 000 U/kg body weight versus vehicle. Treatment was performed 30 min before, and 24 and 48 h after middle cerebral artery occlusion (MCAo) as in Fig. 1a. (b and c) Acute neuronal damage was assessed at 72 h after 30 min MCAo/reperfusion using hematoxylin standard histochemistry. Direct cerebral lesion volumes were determined on five coronal brain sections (approximately interaural 6.6, 5.3, 3.9, 1.9, and −0.1 mm, respectively) by computer-assisted volumetry. Representative images of hematoxylin histochemistry are presented in (c). Number of animals that completed the experiment: vehicle Faim2$^{+/+}$: $n = 7$; vehicle Faim2$^{-/-}$: $n = 6$; EPO-treated Faim2$^{+/+}$: $n = 7$; EPO-treated Faim2$^{-/-}$: $n = 8$. Data shown as mean ± SEM, two-way ANOVA followed by Newman-Keul's *post hoc* test, #$p < 0.05$ relative to wild-type within treatment, scale bar 5 mm.

provided by the manufacturer of the micro-CT (Reconstruction Studio; Yxlon International). A filtered back projection algorithm with Shepp-Logan filter was used for image reconstruction. The matrix for reconstruction was 512 × 512 × 512 voxels.

Phenotyping in the German Mouse Clinic (GMC)

Fifty-nine mice (15 male Faim2$^{-/-}$, 15 female Faim2$^{-/-}$, 14 male Faim2$^{+/+}$, 15 female Faim2$^{+/+}$) were shipped to the German Mouse Clinic (GMC) (www.mouseclinic.de) for extensive, standardized phenotyping. One female (Faim2$^{+/+}$) died during the shipment. GMC evaluated dysmorphology, cardiovascular health, energy metabolism, clinical chemistry, eye, lung function, molecular phenotyping, behavior, neurology, nociception, immunology, and pathology. The phenotypic screen at the GMC was performed according to standardized methods (Gailus-Durner *et al.* 2005, 2009; Fuchs *et al.* 2011). At the GMC, mice were maintained in individually ventilated cages with water and food according to the GMC housing conditions and German laws. All tests performed at the GMC were approved by the responsible authority of the Government of the district government of Upper Bavaria, Germany.

Immunohistochemistry of human brain slices

For immunohistochemistry, human brain tissue from patients who had died from a stroke or its complications was obtained from the RWTH University Neuropathology institute. Brains were fixed in 10% (w/v) paraformaldehyde in phosphate-buffered saline (PBS) and embedded in paraffin. Overall 15 autopsy brains (10 male and 5 female patients, mean age 70.3 and 64.2 years, respectively) with acute ischemic strokes (14 cases with supratentorial ischemic lesions, 1 case with cerebellar acute ischemic stroke) were screened for representative penumbral tissue areas. Coronal sections of 5 μm were mounted on microscope slides and deparaffinized using xylol followed by rehydration with decreasing ethanol series. Antigen-retrieval was performed

for 10 min in the microwave using citric buffer, followed by three washing steps in PBS. Endogenous peroxidase was blocked to reduce unspecific background by incubation with 0.3% (v/v) H_2O_2 in PBS for 30 min followed by three washing steps with PBS. Unspecific antibody binding was reduced by blocking with 3% (v/v) normal goat serum (Vector Laboratories Cat# S-1000, Burlingame, CA, USA) in PBS for 30 min. The primary anti-Faim2 antibody (Sigma-Aldrich Cat# HPA018790, St. Louis, MO, USA, RRID:AB_1852822) was incubated overnight at 4°C in a dilution of 1 : 100 in PBS. The sections were washed again with PBS and secondary antibody (biotinylated goat anti-rabbit IgG, Vector Laboratories Cat# BA-1000, RRID: AB_2313606) was incubated in a dilution of 1 : 200 in PBS for 30 min. Subsequently, the sections were washed and incubated with Avidin-Biotin Complex (Vectastain Elite ABC-Kit, Vector Laboratories Cat# PK-6100) for 30 min, followed by an additional washing step. Visualization of antibody binding was performed via diaminobenzidine (Sigma-Aldrich Cat# 5637) in a dilution of 200 μg/mL in PBS for 10 min. Counterstaining was performed with hemalaun (Merck Millipore Cat# 1.09249, Darmstadt, Germany) and after dehydration sections were coverslipped with Entellan (Merck Millipore Cat# 1.07961).

Experimental design and statistical analysis

Animals were identified by earmark numbers. These numbers were used by a technical assistant not involved in the analysis to randomly assign animals to the experimental groups as shown in Figs 1b and 2a. The surgeon was blinded for genotype. During sample preparation and analysis, the investigators were blinded to genotype and treatment. The infarct volume after 72 h reperfusion time was the primary endpoint of this study. Our study was based on the assumption that a 20% change in the infarct volume is relevant. This required a sample size of eight animals per group (assuming a mean of 50 mm^3 infarct volume after MCAo, standard deviation 16 mm^3, effect size d = 0.625, α = 0.05, Power = 0.2). In total, 36 Faim2$^{+/+}$ and 40 Faim2$^{-/-}$ mice entered into the experiments. The study was not pre-registered.

Data are presented as mean ± SEM with 'n' equal to the number of animals. Power analysis was carried out with G*Power. Statistical analyses were performed using GraphPad Prism 5.0 (GraphPad Software Inc., San Diego, CA, USA). The statistical test used is indicated in the figure legend. The null hypothesis was rejected at the 0.05 level. If not stated otherwise, data that was generated by the German Mouse Clinic was analyzed using R; tests for genotype effects were made using t-test, Wilcoxon rank sum test, linear models, or ANOVA depending on the assumed distribution of the parameter and the questions addressed to the data.

Results

Faim2-deficiency reduced EPO-mediated neuroprotection after MCAo

The impact of Faim2 on the neuroprotective effect of EPO in the context of focal cerebral ischemia was tested by comparing the EPO-mediated reduction in infarct volumes between Faim2$^{-/-}$ and Faim2$^{+/+}$ littermates (Fig. 1c and d). 30 min of MCAo with 72 h reperfusion were combined with the administration of EPO (5000 U/kg body weight) or saline as a control (Vehicle). EPO was administered i.p. 30 min before as well as 24 and 48 h after MCAo (Fig. 1a). None of the analyzed mice displayed atypical neurological deficits, that is, circling, seizure or coma, after MCAo and reperfusion.

As expected and demonstrated in earlier experiments (Reich *et al.* 2011) saline-treated Faim2$^{-/-}$ mice suffered from larger infarct volumes than saline-treated Faim2$^{+/+}$ mice (Fig. 1c and d). EPO treatment (3 × 5000 U/kg body weight) reduced the ischemic lesion volume by 63% in Faim2$^{+/+}$ wild-type mice, but only by 24% in Faim2$^{-/-}$ animals (Fig. 1c). In order to explain the lack of EPO effects in Faim2$^{-/-}$ mice, we quantified erythropoietin receptor (EPO-R) expression using qRT-PCR of brain lysates and found no difference between Faim2$^{-/-}$ and Faim2$^{+/+}$ mice (Fig. 3c and d). Moreover, hematocrit values after EPO application increased in Faim2$^{+/+}$ (fraction length of packed red blood cells: vehicle = 53.3; EPO = 60.2***) as well as in Faim2$^{-/-}$ mice (fraction length of packed red blood cells: vehicle = 48.9; EPO = 55.0***; two-way ANOVA followed by Bonferroni *post hoc* test. *p < 0.001 relative to vehicle treatment within genotype). Thus, Faim2 deficiency blunted the neuroprotective effect of EPO but did not affect the systemic availability of EPO and its effect on hematopoiesis.

Treatment with a higher dosage of EPO is not protective

Neuroprotection by EPO after ischemic stroke is dose-dependent (Wang *et al.* 2007). To investigate EPO's neuroprotective potential under supramaximal EPO conditions, we administered a high dose of EPO (90 000 U/kg body weight) in Faim2 wild-type and Faim2-deficient mice subjected to 30 min of MCAo (Fig. 2). EPO was administered 30 min before as well as 24 and 48 h after MCA occlusion (Fig. 1a). Ischemic lesion volumes in Faim2$^{-/-}$ and Faim2$^{+/+}$ mice after 72 h of reperfusion were compared.

Again, saline-treated Faim2$^{-/-}$ mice showed a larger infarct volume than Faim2$^{+/+}$ mice (Fig. 2b and c), consistent with our previous finding (Reich *et al.* 2011). In both genotypes high-dose EPO did not prevent neuronal loss (Fig. 2b). The infarct volume was comparable to saline-treated ischemic mice with a trend for higher neuronal loss in EPO-treated Faim2$^{+/+}$ animals (Fig. 2b). These results indicate that application of high-dose EPO is not neuroprotective in murine transient cerebral ischemia.
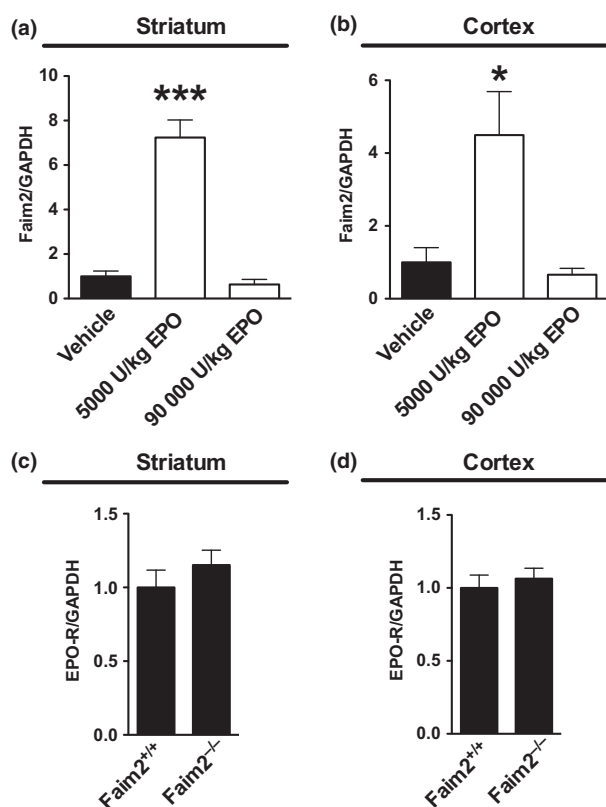
Fig. 3 Erythropoietin (EPO)-dependant Faim2 gene regulation in mouse brain. (a) Striatal and (b) cortical RNA was isolated from wild-type mice 12 h after a single dose of erythropoietin (5000 U/kg, or 90 000 U/kg, respectively) or vehicle. Faim2 transcript abundance was analyzed by quantitative reverse transcription PCR (qRT-PCR) and normalized for GAPDH gene expression. Number of animals: vehicle: $n = 6$; EPO 5000 U/kg: $n = 6$; EPO 90 000 U/kg: $n = 6$. Data shown as mean $\pm$ SEM, one-way ANOVA followed by Bonferroni *post hoc* test. ***$p < 0.0001$, *$p < 0.05$ compared to vehicle, 3 technical replicates per animal. (c) Striatal and (d) cortical RNA was isolated from 12 week-old Faim2$^{-/-}$ and wild-type littermates (Faim2$^{+/+}$). EPO receptor (EPO-R) transcript abundance was analyzed by qRT-PCR and normalized for GAPDH gene expression. Number of animals Faim2$^{+/+}$: $n = 7$; Faim2$^{-/-}$: $n = 7$. Data shown as mean $\pm$ SEM, unpaired *t*-test, 3 technical replicates per animal.

EPO–dependent Faim2 expression in mouse brain

One possible interpretation of the reduced EPO effect in Faim2$^{-/-}$ mice is that Faim2 is part of the neuroprotective signaling cascade initiated by EPO administration. In order to support this hypothesis we tested whether EPO administration regulates Faim2 gene expression in the brain using qRT-PCR.

Faim2 mRNA was increased by the neuroprotective EPO dose (5000 U/kg) in the striatum (Fig. 3a) and in the cortex (Fig. 3b). EPO at the high, non-protective dose (90 000 U/kg) did not change Faim2 expression (Fig. 3a and b). In summary, these findings are consistent with the hypothesis

that up-regulated Faim2 expression contributes to the neuroprotective effect of EPO.

Faim2$^{-/-}$ mice did not reveal a spontaneous phenotype

In order to rule out alternative explanations for the reduced cerebral infarcts and the lacking effects of EPO in Faim2-deficient mice, cohorts of male and female Faim2$^{-/-}$ mice and Faim2$^{+/+}$ littermates were sent to the German Mouse Clinic (GMC) where they were screened for neurological and hematological parameters (Table 1). Subtle, but non-significant differences were found in the auditory brainstem response, motor behavior, eye morphology, fat content, clinical chemistry, and fasting-induced weight loss. As presented in Table 2, there were no genotype or sex-related differences in the analyzed hematological parameters.

Differences and variations within the anatomy of the cerebral macroangiology can influence the execution and the results of the MCAo model. Therefore, mice of both genotypes were subjected to digital subtraction angiography (DSA, Fig. 4a–c) and micro-computed tomography angiography (micro-CTA with maximum intensity projection [MIP]-reconstructions) (Fig. 4d and e).

The results of both examinations showed no gross abnormality of the vascular architecture. This was confirmed by quantifying the vessel diameters of anterior cerebral artery (ACA), middle cerebral artery (MCA), posterior cerebral artery (PCA), internal carotid artery and the basilar artery (BA) (Fig. 4c). Defects of the blood-brain barrier in Faim2$^{-/-}$ mice were not observed by histology (Fig. 4f and g). Taken together, the results of the GMC screen and the DSA/CTA datasets excluded relevant Faim2 genotype-dependent hematological and vascular differences.

Faim2 is differentially expressed in human ischemic penumbra

In order to evaluate the relevance of Faim2 in humans, neocortical brain slices from stroke autopsy cases were stained for Faim2 (Fig. 5).

Cortical regions adjacent to the ischemic brain infarction showed freshly damaged neurons with shrunken and hyper-eosinophilic cytoplasm as revealed by hematoxylin staining (Fig. 5a). These areas showed a strong staining for Faim2 (Fig. 5b and c) including a distribution in neurites (Fig. 5b). Pre-apoptotic neurons displayed a nuclear Faim2 staining pattern (Fig. 5c). On the contrary, Faim2 staining in healthy cortical brain areas was rather faint (Fig. 5d).

Discussion

In this study, we found that low-dose EPO increases Faim2 expression and reduces infarct size in a mouse model of transient cerebral ischemia. In Faim2-deficient mice, there was no significant reduction in infarct size by EPO. A high-EPO dose did not increase Faim2 expression and did not

Table 1 Overview of tests performed by the German Mouse Clinic and summary of results

Screen	Tests	Phenotype summary Faim2$^{-/-}$
Behavior	Pre-pulse Inhibition/Acoustic Startle Reflex	None
	Open Field	None
Neurology	Auditory Brainstem Response	Mild impaired hearing sensitivity
	Grip Strength, Rotarod, Modified SHIRPA, balance beam	Subtle
	Lactate	None
Eye screen	Optical Coherence Tomography	None
	Eye size, Scheimpflug, Virtual Drum, Eye Morphology	Axial eye length decreased; anterior chamber depth decreased; visual function decreased
Metabolic screen	Minispec (NMR)	Fat content trended to be increased
	Indirect Calorimetry (TSE)	None
Clinical chemistry and hematology	Clinical Chemistry (*ad libitum* fed mice)	Slightly decreased plasma urea levels, subtle increase in alpha-amylase activity
	Hematology (Details, see Table 2)	None
	IpGTT	Slightly elevated fasting-induced weight loss, subtle decrease in glucose T0 and elevated AUC 30–120
Immunology screen	Flow Cytometry	None
Allergy screen	Transepidermal water loss	None
Pathology screen	Microscopy (integrity of the blood-brain barrier, testis)	No defects visible (e.g., Fig. 4f–g)

SHIRPA: SmithKline Beecham, Harwell, Imperial College, Royal London Hospital, phenotype assessment; NMR: Nuclear Magnetic Resonance spectroscopy; IpGTT: Intraperitoneal Glucose Tolerance Test; AUC: Area Under the Curve.

Table 2 No genotype related differences in hematological parameters screened by the German Mouse Clinic

	Female		Male		Linear model		
	Faim2$^{+/+}$ n = 14 Mean ± SD	Faim2$^{-/-}$ n = 15 Mean ± SD	Faim2$^{+/+}$ n = 14 Mean ± SD	Faim2$^{-/-}$ n = 15 Mean ± SD	Genotype p-value	Sex p-value	Genotype:Sex p-value
RBC [Mio/mm^3]	10.66 ± 1.08	10.86 ± 0.71	11.12 ± 0.69	11.16 ± 0.59	0.573	0.069	0.705
HGB [g/dl]	16.56 ± 1.68	17.07 ± 0.99	16.79 ± 1.25	16.81 ± 0.81	0.411	0.962	0.436
HCT [%]	50.81 ± 4.89	51.89 ± 3.42	51.71 ± 3.07	51.57 ± 2.31	0.615	0.755	0.509
MCV [fl]	47.86 ± 0.77	48.07 ± 1.1	46.71 ± 0.61	46.2 ± 0.68	0.48	< 0.001	0.097
MCH [pg]	15.54 ± 0.45	15.74 ± 0.5	15.1 ± 0.41	15.06 ± 0.48	0.5	< 0.001	0.317
MCHC [g/dl]	32.58 ± 0.63	32.93 ± 0.79	32.46 ± 0.74	32.6 ± 0.84	0.222	0.265	0.608
RDW [%]	13.56 ± 0.51	13.79 ± 0.62	13.9 ± 0.43	13.95 ± 0.78	0.377	0.114	0.581
WBC [10^3/mm^3]	10.04 ± 3.77	8.73 ± 2.85	13.68 ± 2.78	12.31 ± 2.47	0.095	< 0.001	0.972
PLT [10^3/mm^3]	1143 ± 165.61	1058 ± 198.97	1309 ± 245.12	1331 ± 205.23	0.57	< 0.001	0.329
MPV [fl]	6.23 ± 0.31	6.21 ± 0.21	6.11 ± 0.38	6.04 ± 0.12	0.532	0.047	0.751
PDW [fl]	5.56 ± 0.45	5.49 ± 0.3	5.36 ± 0.41	5.25 ± 0.19	0.294	0.02	0.829
PLCR [%]	2.19 ± 1.31	1.92 ± 0.55	2.22 ± 2.29	1.54 ± 0.37	0.18	0.619	0.563
PCT [%]	0.71 ± 0.11	0.65 ± 0.12	0.79 ± 0.13	0.8 ± 0.13	0.471	0.001	0.311

RBC: red blood cell count; HGB: hemoglobin; HCT: hematocrit; MCV: mean corpuscular volume; MCH: mean corpuscular hemoglobin; MCHC: mean corpuscular hemoglobin concentration; RDW: red blood cell distribution width; WBC: white blood cell count; PLT: platelet count; MPV: mean platelet volume; PDW: platelet distribution width; PLCR: platelet large cell ratio (% of platelets with volume > 12 fl); PCT: plateletcrit (% of whole blood volume made up from platelets).

reduce infarct size. These findings are consistent with the hypothesis that Faim2 up-regulation contributes to the neuroprotective effect of EPO. The relevance of Faim2 regulation for cerebral ischemia in humans is supported by increased Faim2 expression in the penumbra region.

Our first finding is that infarcts following transient MCAo are larger in Faim2-deficient mice than in wild-type mice. This confirms our earlier report (Reich *et al.* 2011). The most likely protective mechanism of Faim2 is the eponymous inhibition of Fas/CD95-induced apoptosis (Beier *et al.* 2005), which is
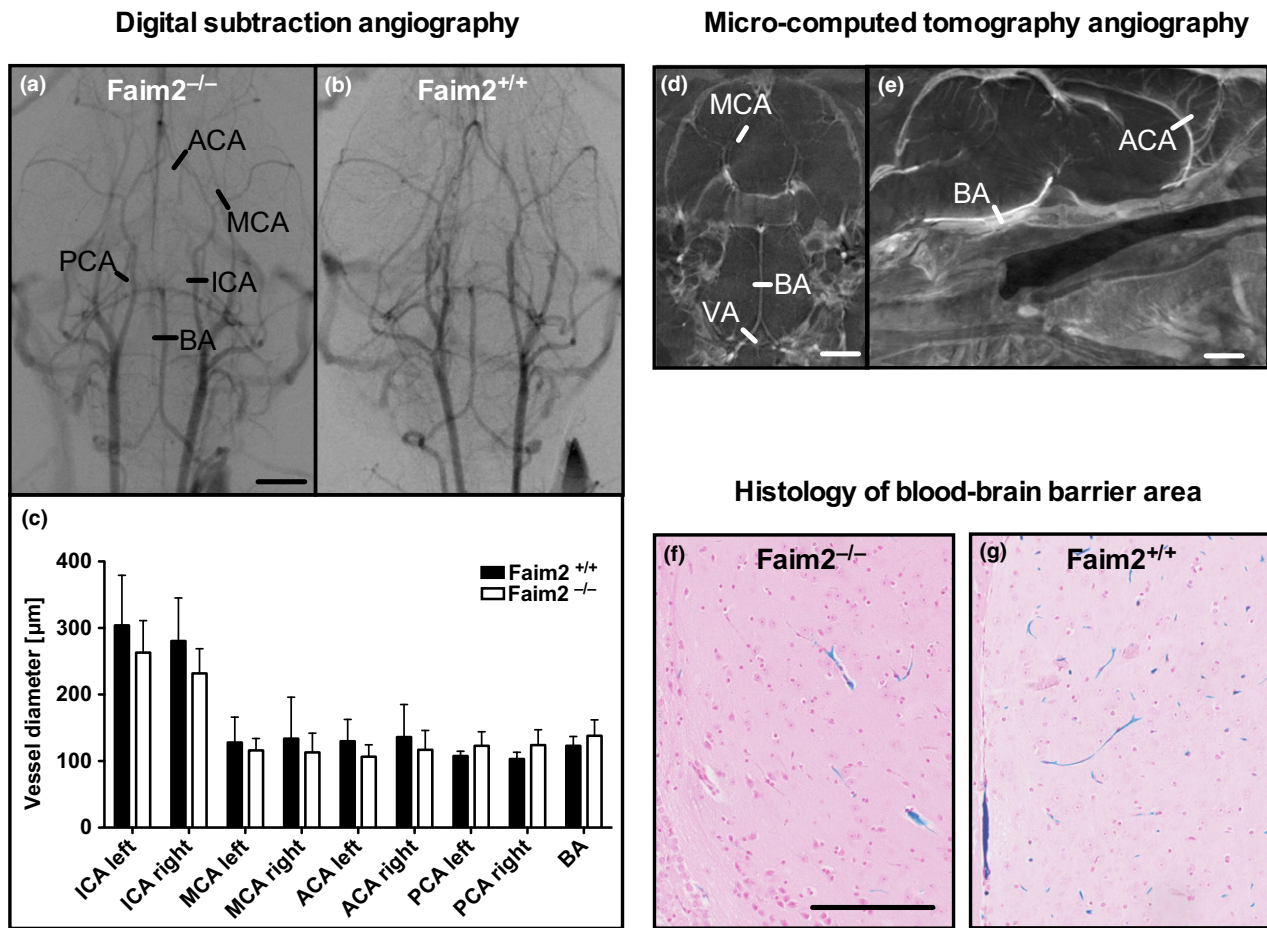
Digital subtraction angiography

Micro-computed tomography angiography

Histology of blood-brain barrier area

Fig. 4 No genotype-related differences in cerebrovascular anatomy. Exemplarily, *in vivo* digital subtraction angiography (DSA) of a Faim2$^{-/-}$ mouse (a) and a Faim2$^{+/+}$ wild-type mouse (b) are shown. Points where vessel diameters where measured are indicated in (a). (c) No differences regarding cerebrovascular anatomy or vessel diameter between Faim2$^{-/-}$ ($n = 5$) and Faim2$^{+/+}$ mice ($n = 4$) were observed. Data shown as mean ± SEM, unpaired *t*-test. (d) and (e) show examples of maximum intensity projection reconstructions of a micro-computed tomography aniography

dataset of a Faim2$^{-/-}$ mouse. ACA: anterior cerebral artery, BA: basilar artery, ICA: internal carotid artery, MCA: middle cerebral artery, PCA: posterior cerebral artery, VA: vertebral artery, scale bar 1 mm. (f) Faim2$^{-/-}$ ($n = 2$) and (g) Faim2$^{+/+}$ ($n = 2$) mice were perfused using 2% (w/v) formalin and 50% (v/v) inc in phospate-buffered saline to display the integrity of the blood-brain barrier. Brains were post fixed in 4% (w/v) formalin for 48 h, paraffin embedded, before 4 μm thick slides were counter-stained with Kernechtrot, scale bar 100 μm.

well documented in the context of cerebral ischemia (Ferrer and Planas 2003; Broughton *et al.* 2009; Reich *et al.* 2011). However, Fas/CD95 signaling does not solely affect cell death in pathological conditions (Reich *et al.* 2008), but can also be important in normal development for example of vascular cells (Stoneman and Bennett 2009). Therefore, relevant differences within the cerebro-vascular architecture between Faim2$^{-/-}$ and wild-type mice had to be ruled out as an alternative explanation for the observed differences in infarct volumes. This was achieved by *in vivo* DSA and CTA (Fig. 4a–e) as well as by a thorough overall phenotype analysis as investigated by the GMC (Tables 1 and 2). In addition, we observed unaltered EPO receptor expression (Fig. 3c and d) and hematological response to EPO in Faim2-deficient mice.

Our second finding is a reduction in infarct size with low-dose EPO. Low-dose EPO significantly reduced infarct size by 63% (Fig. 1c) in wild-type mice. In previous work by Fletcher and colleagues, EPO given at a similar dose (100 U, corresponding to 5000 U/kg for a 20 g mouse) reduced infarct size by only 31%, and this difference did not reach statistical significance because of high variation within the experimental groups (Fletcher *et al.* 2009). We attribute this discrepancy to the shorter occlusion time in our study (30 vs. 60 min) and the longer duration of reperfusion (72 vs. 24 h), which favor an apoptotic cell death mechanism. The shorter time of occlusion also explains the overall smaller infarcts noted in our studies as compared to the cited study by Fletcher and colleagues (Fletcher *et al.* 2009). Using the
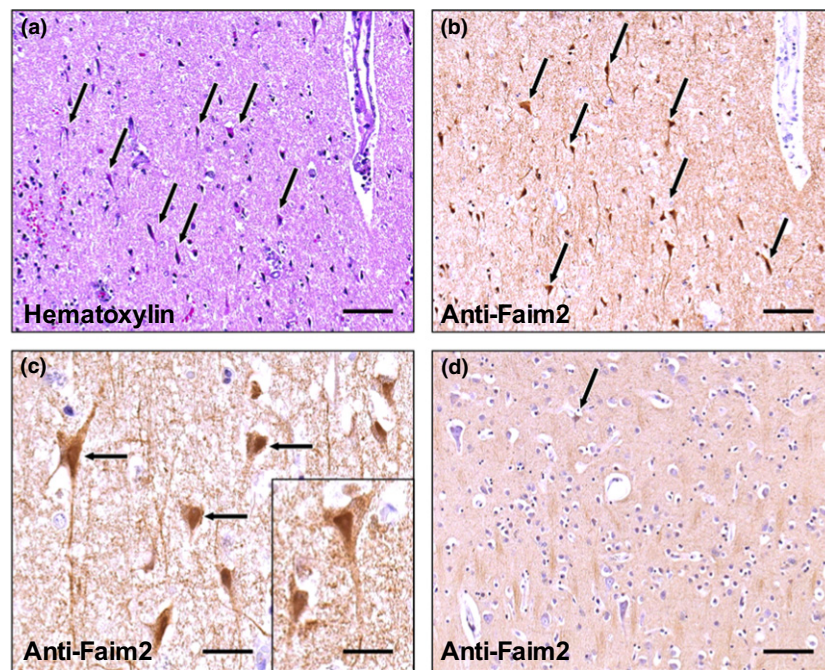
Fig. 5 Faim2 is differentially expressed in the human ischemic penumbra. (a) Selective neuronal damage in the vicinity of a stadium I – II ischemic brain infarct (autopsy case, female patient, 69 year). Some freshly damaged cortical neurons with shrunken and hypereosinophilic cytoplasm are indicated by arrows (Hematoxylin stain; scale bar = 90 μm). (b) Immunohistochemical staining with anti-Faim2 highlighting several ischemic neuronal cells. Note the prominent staining in some cells (same area as in a; Faim2 antibody from Sigma Aldrich; HPA 018790; scale bar = 90 μm). (c) Damaged though not always shrunken Faim2-positive neurons show a predominant nuclear staining pattern (same case as in a and b; Faim2 immunostaining; scale bar = 28 μm, scale bar inset = 19 μm). (d) Non-ischemic neocortical area (autopsy material). Only very few scattered cells show faint reactivity with Faim2 antibody (scale bar = 90 μm).

same experimental paradigm we did not observe reduced infarct size with the high dose of EPO (Fig. 2b). This dose-dependency may explain some of the inconsistencies in the literature on the neuroprotective effects of EPO in stroke models.

The mechanism by which EPO protects neurons in cerebral ischemia is not known. Infarct size in MCAo is strongly affected by the amount of cell death in the penumbra (Fisher and Bastan 2012), which primarily occurs through apoptosis (Broughton *et al.* 2009; Chelluboina *et al.* 2014). Since EPO increases Faim2 expression in a dose-dependent manner and Faim2 decreases apoptotic cell death, it is plausible to hypothesize that Faim2 contributes to the protective effect of EPO. In Faim2$^{+/+}$ mice, the low dose of EPO increased Faim2 expression and significantly reduced the infarct size after transient MCAo. The high dose of EPO did not increase Faim2 expression and did not reduce the infarct size. Either dose of EPO failed to significantly reduce the infarct size in Faim2-deficient mice. These findings are consistent with the hypothesis that Faim2 contributes to the protective effect of EPO. The hypothesis is also consistent with the reduction in apoptosis observed with EPO in MCAo models (Wang *et al.* 2007). Unaltered hematological parameters (Table 2), unaltered EPO receptor expression in the brain (Fig. 3c and d), and the absence of visible blood-brain barrier differences (Fig. 4f and g) make it unlikely that Faim2 acts upstream of EPO signaling. Previous findings that EPO signals through the PI3K/Akt pathway (Ghezzi and Brines 2004) and that Faim2 promoter activity is regulated by Akt (Beier *et al.* 2005) suggest a neuroprotective signaling cascade in the ischemic penumbra consisting of EPO, EPO receptor, PI3K, Akt, and Faim2. Yet, further research is required to confirm this pathway.

The therapeutic potential of EPO has already been tested in clinical trials. Ehrenreich and colleagues were the first to report clinical outcome in patients that received 33 000 U/50 mL/30 min intravenously (i.v.), in a therapeutic window of 8 h after acute ischemic stroke, and again 24 and 48 h later (cumulative EPO doses of 100 000 U) without relevant safety concerns (Ehrenreich *et al.* 2002). This was in line with a meta-analysis by Minnerup (Minnerup *et al.* 2009). In the follow-up study, stroke patients receiving a slightly higher EPO dose (40 000 U/50 mL/30 min, i.v. < 6 h after symptom onset, and again 24 and 48 h later, cumulative EPO dose 120 000 U) were found to die more often because of thromboembolic complications (Ehrenreich *et al.* 2009).

Post-analysis indicates that patients without rtPA thrombolysis benefit from EPO treatment (Ehrenreich *et al.* 2009). Potential negative effects of dual treatment with EPO and thrombolysis (rtPA) after stroke have already been shown in preclinical trials (Jia *et al.* 2010; Zechariah *et al.* 2010). Considerable advancement has been made in improving reperfusion therapy for stroke patients (Goyal *et al.* 2016; Hankey 2017). Yet, we are still missing neuroprotective strategies, which among other benefits could prolong the therapeutic window for reperfusion therapies. Therefore, the therapeutic potential of EPO should be reconsidered, especially in the context of successful endovascular reperfusion treatment of patients with large vessel occluding acute ischemic stroke. However, EPO has to be investigated with respect to dose, timing and contraindications as well as receptor subtype selectivity and distribution (Leist *et al.* 2004). Our finding of a lacking effect of high-dose EPO together with the second clinical trial (Ehrenreich *et al.* 2009) indicate that a lower dose of EPO could be more beneficial. Furthermore, our finding that Faim2 may contribute to EPO-induced neuroprotection suggests that measuring Faim2 expression could be helpful to determine an optimal dosing regimen for EPO.

The relevance of Faim2 for infarct size in humans is confirmed by our findings in human autopsy samples. They show, however, a higher Faim2 immunostaining in the so-called penumbra, the area adjacent to an ischemic infarct (Fig. 5). In our earlier study in mice we reported decreased Faim2 mRNA expression in the core of the infarct after MCAo (Reich *et al.* 2011). In contrast to the ischemic infarct core, penumbral tissue benefits from vascular integrity and may benefit from Faim2 regulation protecting cells from apoptosis. Indeed, differential Faim2 expression is consistent with a hypothesis laid out previously (Reich *et al.* 2008) speculating on a Faim2-mediated involvement of Fas/CD95 in neuronal apoptosis and regeneration. In this hypothesis, dynamic spatio-temporal Faim2 expression allows for neuroprotection by increased Faim2 expression and inhibition of Fas/CD95-induced apoptosis during the acute phase of a disease and in areas of salvable tissue, whereas decreased Faim2 after the insult or in other areas of the brain may allow regeneration through alternative Fas/CD95 signaling.

We confirm that Faim2 is neuroprotective in a mouse model of transient focal cerebral ischemia. At least partly, Faim2 appears to mediate the protective effects of EPO. However, the effects of EPO are dose-dependent. Furthermore work dissecting the signaling pathway between EPO and Faim2 may allow improvement of EPO dosing regimens maximizing Faim2 expression and minimizing side effects. Given that protective effects of Faim2 were also observed in models of bacterial meningitis (Tauber *et al.* 2014), Parkinson disease (Komnig *et al.* 2016) and retinal detachment (Besirli *et al.* 2012), an improved EPO regimen could be applied not only for stroke but also for further neurologic diseases.

Conclusions

This study demonstrated that the neuroprotective effects of EPO are dose-dependent, and that Faim2 may contribute to the neuroprotective effects of EPO. Furthermore work on the EPO signaling pathway may allow improvement of dosing regimens and revitalize neuroprotective approaches for stroke patients and for patients with further neurologic diseases. The recent success of endovascular stroke treatment indicates that translation from bench-to-bedside of neuroprotective strategies derived in murine occlusion/reperfusion models is more promising than ever.

Acknowledgements and conflict of interest disclosure

References

Beier C. P., Wischhusen J., Gleichmann M. *et al.* (2005) FasL (CD95L/APO-1L) resistance of neurons mediated by phosphatidylinositol 3-kinase-Akt/protein kinase B-dependent expression of lifeguard/neuronal membrane protein 35. *J. Neurosci.* **25**, 6765–6774.

Besirli C. G., Zheng Q. D., Reed D. M. and Zacks D. N. (2012) ERK-mediated activation of Fas apoptotic inhibitory molecule 2 (Faim2) prevents apoptosis of 661W cells in a model of detachment-induced photoreceptor cell death. *PLoS ONE* **7**, e46664.

Brines M. L., Ghezzi P., Keenan S., Agnello D., de Lanerolle N. C., Cerami C., Itri L. M. and Cerami A. (2000) Erythropoietin crosses the blood-brain barrier to protect against experimental brain injury. *Proc. Natl Acad. Sci. USA* **97**, 10526–10531.

Broughton B. R., Reutens D. C. and Sobey C. G. (2009) Apoptotic mechanisms after cerebral ischemia. *Stroke* **40**, e331–e339.

Brunet A., Datta S. R. and Greenberg M. E. (2001) Transcription-dependent and -independent control of neuronal survival by the PI3K-Akt signaling pathway. *Curr. Opin. Neurobiol.* **11**, 297–305.

Chateauvieux S., Grigorakaki C., Morceau F., Dicato M. and Diederich M. (2011) Erythropoietin, erythropoiesis and beyond. *Biochem. Pharmacol.* **82**, 1291–1303.

Chelluboina B., Klopfenstein J. D., Gujrati M., Rao J. S. and Veeravalli K. K. (2014) Temporal regulation of apoptotic and anti-apoptotic molecules after middle cerebral artery occlusion followed by reperfusion. *Mol. Neurobiol.* **49**, 50–65.

Dirnagl, Ulrich and Group, Members of the MCAO-SOP. Standard operating procedures (SOP) in experimental stroke research: SOP for middle cerebral artery occlusion in the mouse. Available from Nature Precedings.

Ehrenreich H., Hasselblatt M., Dembowski C. *et al.* (2002) Erythropoietin therapy for acute stroke is both safe and beneficial. *Mol. Med.* **8**, 495–505.

Ehrenreich H., Weissenborn K., Prange H. *et al.* (2009) Recombinant human erythropoietin in the treatment of acute ischemic stroke. *Stroke* **40**, e647–e656.

Fernandez M., Segura M. F., Sole C., Colino A., Comella J. X. and Cena V. (2007) Lifeguard/neuronal membrane protein 35 regulates Fas ligand-mediated apoptosis in neurons via microdomain recruitment. *J. Neurochem.* **103**, 190–203.

Ferrer I. and Planas A. M. (2003) Signaling of cell death and cell survival following focal cerebral ischemia: life and death struggle in the penumbra. *J. Neuropathol. Exp. Neurol.* **62**, 329–339.

Figueiredo G., Brockmann C., Boll H., Heilmann M., Schambach S. J., Fiebig T., Kramer M., Groden C. and Brockmann M. A. (2012) Comparison of digital subtraction angiography, micro-computed tomography angiography and magnetic resonance angiography in the assessment of the cerebrovascular system in live mice. *Clin. Neuroradiol.* **22**, 21–28.

Fisher J. W. (2010) Landmark advances in the development of erythropoietin. *Exp. Biol. Med. (Maywood)* **235**, 1398–1411.

Fisher M. and Bastan B. (2012) Identifying and utilizing the ischemic penumbra. *Neurology* **79**, S79–S85.

Fletcher L., Kohli S., Sprague S. M., Scranton R. A., Lipton S. A., Parra A., Jimenez D. F. and Digicaylioglu M. (2009) Intranasal delivery of erythropoietin plus insulin-like growth factor-I for acute neuroprotection in stroke. Laboratory investigation. *J. Neurosurg.* **111**, 164–170.

Fuchs H., Gailus-Durner V., Adler T. *et al.* (2011) Mouse phenotyping. *Methods* **53**, 120–135.

Gailus-Durner V., Fuchs H., Becker L. *et al.* (2005) Introducing the German Mouse Clinic: open access platform for standardized phenotyping. *Nat. Methods* **2**, 403–404.

Gailus-Durner V., Fuchs H., Adler T. *et al.* (2009) Systemic first-line phenotyping. *Methods Mol. Biol.* **530**, 463–509.

Gertz K., Kronenberg G., Kalin R. E. *et al.* (2012) Essential role of interleukin-6 in post-stroke angiogenesis. *Brain* **135**, 1964–1980.

Ghezzi P. and Brines M. (2004) Erythropoietin as an antiapoptotic, tissue-protective cytokine. *Cell Death Differ.* **11**(Suppl 1), S37–S44.

Goyal M., Menon B. K., van Zwam W. H. *et al.* (2016) Endovascular thrombectomy after large-vessel ischaemic stroke: a meta-analysis of individual patient data from five randomised trials. *Lancet* **387**, 1723–1731.

Hankey G. J. (2017) Stroke. *Lancet* **389**, 641–654.

Jia L., Chopp M., Zhang L., Lu M. and Zhang Z. (2010) Erythropoietin in combination with tissue plasminogen activator exacerbates brain hemorrhage when treatment is initiated 6 hours after stroke. *Stroke* **41**, 2071–2076.

Kilic E., Dietz G. P., Hermann D. M. and Bahr M. (2002) Intravenous TAT-Bcl-Xl is protective after middle cerebral artery occlusion in mice. *Ann. Neurol.* **52**, 617–622.

Kilic E., Kilic U., Soliz J., Bassetti C. L., Gassmann M. and Hermann D. M. (2005) Brain-derived erythropoietin protects from focal cerebral ischemia by dual activation of ERK-1/-2 and Akt pathways. *FASEB J.* **19**, 2026–2028.

Kim A. S., Cahill E. and Cheng N. T. (2015) Global stroke belt: geographic variation in stroke burden worldwide. *Stroke* **46**, 3564–3570.

Komnig D., Schulz J. B., Reich A. and Falkenburger B. H. (2016) Mice lacking Faim2 show increased cell death in the MPTP mouse model of Parkinson disease. *J. Neurochem.* **139**, 848–857.

Leist M., Ghezzi P., Grasso G. *et al.* (2004) Derivatives of erythropoietin that are tissue protective but not erythropoietic. *Science* **305**, 239–242.

Lu Y. M., Tao R. R., Huang J. Y., Li L. T., Liao M. H., Li X. M., Fukunaga K., Hong Z. H. and Han F. (2012) P2X7 signaling promotes microsphere embolism-triggered microglia activation by maintaining elevation of Fas ligand. *J. Neuroinflammation* **9**, 172.

Minnerup J., Heidrich J., Rogalewski A., Schabitz W. R. and Wellmann J. (2009) The efficacy of erythropoietin and its analogues in animal stroke models: a meta-analysis. *Stroke* **40**, 3113–3120.

Pundik S., Xu K. and Sundararajan S. (2012) Reperfusion brain injury: focus on cellular bioenergetics. *Neurology* **79**, S44–S51.

Reich A., Spering C. and Schulz J. B. (2008) Death receptor Fas (CD95) signaling in the central nervous system: tuning neuroplasticity? *Trends Neurosci.* **31**, 478–486.

Reich A., Spering C., Gertz K. *et al.* (2011) Fas/CD95 regulatory protein Faim2 is neuroprotective after transient brain ischemia. *J. Neurosci.* **31**, 225–233.

Sanderson T. H., Reynolds C. A., Kumar R., Przyklenk K. and Huttemann M. (2013) Molecular mechanisms of ischemia-reperfusion injury in brain: pivotal role of the mitochondrial membrane potential in reactive oxygen species generation. *Mol. Neurobiol.* **47**, 9–23.

Schambach S. J., Bag S., Steil V., Isaza C., Schilling L., Groden C. and Brockmann M. A. (2009) Ultrafast high-resolution in vivo volume-CTA of mice cerebral vessels. *Stroke* **40**, 1444–1450.

Schweitzer B., Taylor V., Welcher A. A., McClelland M. and Suter U. (1998) Neural membrane protein 35 (NMP35): a novel member of a gene family which is highly expressed in the adult nervous system. *Mol. Cell Neurosci.* **11**, 260–273.

Siren A. L., Knerlich F., Poser W., Gleiter C. H., Bruck W. and Ehrenreich H. (2001) Erythropoietin and erythropoietin receptor in human ischemic/hypoxic brain. *Acta Neuropathol.* **101**, 271–276.

Somia N. V., Schmitt M. J., Vetter D. E., Van Antwerp D., Heinemann S. F. and Verma I. M. (1999) LFG: an anti-apoptotic gene that provides protection from Fas-mediated cell death. *Proc. Natl Acad. Sci. USA* **96**, 12667–12672.

Stoneman V. E. and Bennett M. R. (2009) Role of Fas/Fas-L in vascular cell apoptosis. *J. Cardiovasc. Pharmacol.* **53**, 100–108.

Tauber S. C., Harms K., Falkenburger B. H., Weis J., Sellhaus B., Nau R., Schulz J. B. and Reich A. (2014) Modulation of hippocampal neuroplasticity by Fas/CD95 regulatory protein 2 (Faim2) in the course of bacterial meningitis. *J. Neuropathol. Exp. Neurol.* **73**, 2–13.

Villa P., Bigini P., Mennini T. *et al.* (2003) Erythropoietin selectively attenuates cytokine production and inflammation in cerebral ischemia by targeting neuronal apoptosis. *J. Exp. Med.* **198**, 971–975.

Wakida K., Shimazawa M., Hozumi I., Satoh M., Nagase H., Inuzuka T. and Hara H. (2007) Neuroprotective effect of erythropoietin, and

role of metallothionein-1 and -2, in permanent focal cerebral ischemia. *Neuroscience* **148**, 105–114.

Wang Y., Zhang Z. G., Rhodes K. *et al.* (2007) Post-ischemic treatment with erythropoietin or carbamylated erythropoietin reduces infarction and improves neurological outcome in a rat model of focal cerebral ischemia. *Br. J. Pharmacol.* **151**, 1377–1384.

Yildirim F., Ji S., Kronenberg G. *et al.* (2014) Histone acetylation and CREB binding protein are required for neuronal resistance against ischemic injury. *PLoS ONE* **9**, e95465.

Yu Y. P., Xu Q. Q., Zhang Q., Zhang W. P., Zhang L. H. and Wei E. Q. (2005) Intranasal recombinant human erythropoietin protects rats against focal cerebral ischemia. *Neurosci. Lett.* **387**, 5–10.

Zechariah A., ElAli A. and Hermann D. M. (2010) Combination of tissue-plasminogen activator with erythropoietin induces blood-brain barrier permeability, extracellular matrix disaggregation, and DNA fragmentation after focal cerebral ischemia in mice. *Stroke* **41**, 1008–1012.